

Simultaneous Nonlinear Model Predictive Control and State Estimation [★]

David A. Copp ^a, João P. Hespanha ^a,

^a *University of California, Santa Barbara, CA 93106-9560, U.S.A.*

Abstract

An output-feedback approach to model predictive control that combines state estimation and control into a single min-max optimization is introduced for discrete-time nonlinear systems. Specifically, a criterion that involves finite forward and backward horizons is minimized with respect to control input variables and is maximized with respect to the unknown initial state as well as disturbance and measurement noise variables. Under appropriate assumptions that encode controllability and observability, we show that the state of the closed-loop remains bounded and that a bound on tracking error can be found for trajectory-tracking problems. We also introduce a primal-dual interior-point method that can be used to efficiently solve the min-max optimization problem and show in simulation examples that the method succeeds even for severely nonlinear and non-convex problems.

Key words: model predictive control; output feedback control; control of constrained systems; optimal control; optimal estimation; algorithms and software.

1 Introduction

Online optimization has become a ubiquitous approach for solving control and estimation problems in both academia and industry. This is largely due to the ability to explicitly accommodate hard state and input constraints in online optimization techniques. Because of this, an especially popular online optimization control technique called model predictive control (MPC) is used in numerous industrial applications (Qin & Badgwell, 2003), and, consequently, much effort has been devoted to developing a stability theory for MPC (see e.g. Camacho & Bordons (2004); Grüne & Pannek (2011); Morari & H Lee (1999); Rawlings (2000); Rawlings & Mayne (2009)). An overview of recent developments can be found in Mayne (2014).

MPC involves the solution of an open-loop optimal control problem at each sampling time. Each of these optimizations results in a sequence of future optimal control actions and a sequence of corresponding future states. The first control action in the sequence is applied to the plant, and then the optimization is solved again at the next sampling time. MPC has historically been popu-

lar for problems in which the plant dynamics are sufficiently slow so that the optimization can be solved between consecutive sampling times. However, as available computational power increases and optimization algorithms improve in terms of speed, MPC can be applied to broader application areas.

MPC is often formulated assuming that the full state of the process to be controlled can be measured. However, this is not possible in many practical cases, so the use of independent algorithms for state-estimation, including observers, filters, and moving horizon estimation (MHE), as discussed, i.e., in Rawlings & Bakshi (2006), is required. Of these methods, MHE is especially attractive for use with MPC because it can be formulated as a similar online optimization problem that explicitly handles constraints. Solving the MHE problem produces a state estimate that is compatible with a set of past measurements that recedes as the current time advances. This estimate is optimal in the sense that it maximizes a criterion that captures the likelihood of the measurements. By receding the set of measurements considered in the MHE optimization, one maintains a constant computational cost for the optimization.

In this paper, we propose an approach to combine MPC and MHE into a single optimization that is solved online to construct an output-feedback controller. To account

[★] Corresponding author D. A. Copp.

Email addresses: `dacopp@engr.ucsb.edu` (David A. Copp), `hespanha@ece.ucsb.edu` (João P. Hespanha).

for the uncertainty that results from unmeasured disturbances and measurement noise, we replace the minimization that is used in classical MPC by a min-max optimization. In this case, the minimization is carried out with respect to future control actions, and the maximization is taken with respect to the variables that cannot be measured, namely the system’s initial state, the unmeasured disturbances, and the output measurement noise. The criterion for this min-max optimization combines a term that captures the control objective and a term that captures the likelihood of the uncertain variables, resulting in essentially the summation of an MPC criterion with an MHE criterion.

The main technical contribution of this paper addresses the stability of the proposed combined MPC/MHE approach. We show that the proposed output-feedback controller results in closed-loop trajectories along which the state of the process remains bounded, and, for tracking problems, our results provide explicit bounds on the tracking error. These results rely on three key assumptions: The first assumption requires the existence of saddle-point equilibria for the min-max optimization, or equivalently, that the min and max commute. In practice, this assumption can be viewed as a form of observability of the process. The second key assumption requires the optimization criterion to include a terminal cost that is a control ISS-Lyapunov function with respect to the disturbance input. This type of assumption is common in classical state-feedback robust MPC. The final observability assumption essentially requires that the backwards horizon is sufficiently large so that enough information about the initial state is obtained in order to find past estimates that are compatible with the dynamics.

A second contribution of this paper is a new primal-dual interior-point algorithm that can be used to compute the saddle-point equilibrium that needs to be solved for online at each sampling time. This algorithm relies on the use of Newton’s method to solve a relaxed version of the Karush-Kuhn-Tucker (KKT) conditions associated with the coupled optimizations that define the saddle-point equilibrium. As in classical primal-dual methods, we replace the equality to zero of the complementary slackness conditions by equality to a positive constant μ that we force to converge to zero as the Newton iterations progress. In practice, the algorithm will stop with a positive value for μ , but we show that this still leads to an ϵ -saddle-point, where ϵ can be explicitly computed and made arbitrarily small through the selection of an appropriate stopping criterion.

1.1 Related Work

State-feedback MPC is a mature field with numerous contributions. Particularly relevant to the results in this paper is the work on the so-called robust or min-max

MPC, which considers model uncertainty, input disturbances, and noise (Bemporad & Morari, 1999; Campo & Morari, 1987; Lee & Yu, 1997; Magni, De Nicolao, Scatoloni & Allgöwer, 2003). Min-max MPC for constrained linear systems was considered by Sockaert & Mayne (1998) and Bemporad, Borrelli & Morari (2003), and a game theoretic approach for robust constrained nonlinear MPC was proposed by Chen, Scherer & Allgöwer (1997). More recent studies of input-to-state stability of min-max MPC can be found in Lazar, Muñoz de la Peña, Heemels & Alamo (2008); Limon, Alamo, Raimondo, de la Peña, Bravo, Ferramosca & Camacho (2009); Raimondo, Limon, Lazar, Magni & Camacho (2009). These works focused on state-feedback MPC and did not consider robustness with respect to errors in state estimation. A novelty of the work presented in this paper is the reliance on saddle-point equilibria, rather than a simple min-max optimal, which we found instrumental in establishing our stability results.

Fewer results are available for output-feedback MPC. An overview of nonlinear output-feedback MPC is given by Findeisen, Imsland, Allgöwer & Foss (2003) and the references therein. Many of these output-feedback approaches involve designing separate state estimator and MPC schemes. Several of the observers, estimators, and filters that have been proposed for use with nonlinear output-feedback MPC include an extended Kalman filter (Huang, Patwardhan & Biegler, 2009), optimization based moving horizon observers (Michalska & Mayne, 1995), high gain observers (Imsland, Findeisen, Bullinger, Allgöwer & Foss, 2003), extended observers (Roset, Lazar, Nijmeijer & Heemels, 2006), and robust MHE (Zhang & Liu, 2013). In contrast to solving the estimation and control problems separately, the formulation of our combined MPC/MHE approach as a single optimization facilitates the stability analysis of the closed-loop without the need for a separation principle for nonlinear systems.

Results on robust output-feedback MPC for constrained, linear, discrete-time systems with bounded disturbances and measurement noise can be found in Mayne, Raković, Findeisen & Allgöwer (2006, 2009), where a stable Luenberger observer is employed for state estimation and robustly stabilizing tube-based MPC is performed to control the state of the observer. Alternatively, in Sui, Feng & Hovd (2008), MHE is employed for state estimation and is combined with a similar tube-based MPC approach. These approaches first solve the estimation problem and show convergence of the state estimate to a bounded set and then take the uncertainty of the state estimate into account when solving the robust MPC problem. The work of Löfberg (2002) combines an estimation scheme, which provides a guaranteed ellipsoidal error bound on the state estimate, with a min-max MPC scheme for estimation and control of linear systems with bounded disturbances and measurement noise.

During the same time that many important results on MPC were developed, parallel work began on MHE. The work of Allgöwer, Badgwell, Qin, Rawlings & Wright (1999) gives a tutorial overview and background of both MPC and MHE as well as methods that can be used to solve these optimization problems. Useful overviews of constrained linear and nonlinear MHE can be found in Rao, Rawlings & Lee (2001) and Rao, Rawlings & Mayne (2003) where, with appropriate assumptions regarding observability, continuity, and an approximate arrival cost, the authors prove asymptotic stability as well as bounded stability in the presence of bounded noise.

More recent results regarding MHE for discrete-time nonlinear systems are given by Alessandri, Baglietto & Battistelli (2008), in which the authors minimize a quadratic cost that includes the standard output error term as well as a term penalizing the distance of the current estimated state from its prediction. The authors prove boundedness of the estimation error, when considering bounded disturbances and measurement noise, and convergence of the state estimate to the true value in the noiseless case. Even more recent work on robust MHE for nonlinear systems appeared in Liu (2013), where first a high-gain observer is used to bound the estimation error, and then that bound is used to design a constraint for incorporation in an MHE problem. This formulation seems to reduce the sensitivity of the performance of MHE to the accuracy of the approximate arrival cost, and boundedness of the state estimate is proven when the noise is bounded.

The optimization algorithm proposed here is heavily inspired by primal-dual interior-point methods (Wright, 1997b) that have been very successful in solving convex optimizations (Boyd & Vandenberghe, 2004). The use of interior-point algorithms to solve MPC problems is discussed by Rao, Wright & Rawlings (1998), and additional early work on efficient numerical methods for solving MPC problems can be found in Biegler (2000); Biegler & Rawlings (1991); Wright (1997a). An overview of the numerical methods available for solving the optimization problems that arise in nonlinear MPC and MHE is given by Diehl, Ferreau & Haverbeke (2009), whereas the more recent work Wang & Boyd (2010) is focused on the development of fast dedicated solvers for MPC problems. A recent survey on sensitivity-based nonlinear programming methods for solving MHE and MPC problems is given in Biegler (2013). In de la Peña, Alamo, Ramírez & Camacho (2007), the authors specifically consider numerical methods for solving min-max MPC as a quadratic program, and robust dynamic programming for min-max MPC of constrained uncertain systems is considered by Diehl & Bjornberg (2004). Finally, the method that is described in Section 5 is directly inspired by the primal-dual interior-point method for a single optimization described in Vandenberghe (2010).

The combined MPC/MHE approach considered here was introduced for the first time in the conference paper by Copp & Hespanha (2014) with neither a stability proof nor a numerical algorithm that could be used to compute the required saddle-point equilibria.

Paper Organization

The remainder of this paper is organized as follows: In Section 2 we formulate the estimation and control problem, and in Section 3 we analyze its closed-loop stability. In Section 4, we discuss the computation of the optimal control through the solution of a pair of coupled optimizations, and in Section 5 we present a primal-dual interior-point method that can be used to solve these optimizations. Finally, we use this method to simulate a nonlinear example in Section 6 and discuss conclusions and future work in Section 7.

2 Problem Formulation

This paper considers the control of a time-varying nonlinear discrete-time process of the form

$$x_{t+1} = f_t(x_t, u_t, d_t), \quad y_t = g_t(x_t) + n_t, \quad \forall t \in \mathbb{Z}_{\geq 0} \quad (1)$$

with *state* $x_t \in \mathcal{X} \subset \mathbb{R}^{n_x}$. The inputs to this system are the *control input* u_t that must be restricted to the bounded set $\mathcal{U} \subset \mathbb{R}^{n_u}$, the *unmeasured disturbance* d_t that is known to belong to the bounded set $\mathcal{D} \subset \mathbb{R}^{n_d}$, and the *measurement noise* n_t that is known to belong to the bounded set $\mathcal{N} \subset \mathbb{R}^{n_y}$. The signal $y_t \in \mathbb{R}^{n_y}$ denotes the *measured output* that is available for feedback. The *control objective* is to select the control signal $u_t \in \mathcal{U}$, $\forall t \in \mathbb{Z}_{\geq 0}$, so as to minimize a criterion of the form

$$\sum_{t=0}^{\infty} c_t(x_t, u_t, d_t) - \sum_{t=0}^{\infty} \eta_t(n_t) - \sum_{t=0}^{\infty} \rho_t(d_t), \quad (2)$$

for worst-case values of the unmeasured disturbance $d_t \in \mathcal{D}$, $\forall t \in \mathbb{Z}_{\geq 0}$, and measurement noise $n_t \in \mathbb{R}^{n_y}$, $\forall t \in \mathbb{Z}_{\geq 0}$. The functions $c_t(\cdot)$, $\eta_t(\cdot)$, and $\rho_t(\cdot)$ in (2) are all assumed to take non-negative values. One can view the terms $\rho_t(\cdot)$ and $\eta_t(\cdot)$ as measures of the likelihood of specific values for d_t and n_t . Then, the negative signs in front of $\rho_t(\cdot)$ and $\eta_t(\cdot)$ penalize the maximizer for using low likelihood values for the disturbances and noise (low likelihood meaning very large values for $\rho_t(\cdot)$ and $\eta_t(\cdot)$).

To better understand (2), it is also useful to note that boundedness of the criterion (2) by a constant γ guarantees that

$$\sum_{t=0}^{\infty} c_t(x_t, u_t, d_t) \leq \gamma + \sum_{t=0}^{\infty} \eta_t(n_t) + \sum_{t=0}^{\infty} \rho_t(d_t). \quad (3)$$

While the results presented here are general, the reader is encouraged to consider the quadratic case $c_t(x_t, u_t, d_t) := \|x_t\|^2 + \|u_t\|^2$, $\eta_t(n_t) := \|n_t\|^2$, $\rho_t(d_t) := \|d_t\|^2$ to gain intuition on the results. In this case, (3) would guarantee that the state x_t and input u_t are ℓ_2 , provided that the disturbance d_t and noise n_t are also ℓ_2 . This would mean that the closed-loop has a finite ℓ_2 -induced gain.

2.1 Finite-Horizon Online Optimization

To overcome the conservativeness of an open-loop control, we use online optimization to generate the control signals. Specifically, at each time $t \in \mathbb{Z}_{\geq 0}$, we compute the control u_t so as to minimize a *finite-horizon* criterion of the form

$$\sum_{s=t}^{t+T-1} c_s(x_s, u_s, d_s) + q_{t+T}(x_{t+T}) - \sum_{s=t-L}^t \eta_s(n_s) - \sum_{s=t-L}^{t+T-1} \rho_s(d_s) \quad (4)$$

under worst-case assumptions on the *unknown* system's initial condition x_{t-L} , unmeasured disturbances d_s , and measurement noise n_s , subject to the constraints imposed by the system dynamics and the measurements y_s collected up to the current time t .

For computational tractability, in (4) we have replaced the infinite summations that appeared in (2) by finite forward and backward horizon lengths. In particular, (4) includes $T \in \mathbb{Z}_{\geq 1}$ future terms of the running cost $c_s(x_s, u_s, d_s)$, which recede as the current time t advances, and $L + 1 \in \mathbb{Z}_{\geq 1}$ past terms of the noise penalty term $\eta_s(n_s)$. The function $q_{t+T}(x_{t+T})$ acts as a terminal cost to penalize the "final" state at time $t + T$.

Since the goal is to optimize (4) at the current time t to compute the control inputs at times $s \geq t$, there is no point in penalizing the running cost $c_s(x_s, u_s, d_s)$ for past time instants $s < t$, which explains the fact that the first summation in (4) starts at time t . There is also no point in considering the values of future measurement noise at times $s > t$, as they will not affect choices made at time t , which explains the fact that the second summation in (4) stops at time t . However, we do need to consider all values for the unmeasured disturbance d_s , because past values affect the (unknown) current state x_t , and future values affect the future values of the running cost.

We denote the sets of non-negative real numbers and non-negative integers as $\mathbb{R}_{\geq 0}$ and $\mathbb{Z}_{\geq 0}$, respectively. Given a discrete-time signal $z : \mathbb{Z}_{\geq 0} \rightarrow \mathbb{R}^n$ and two times $t_0, t \in \mathbb{Z}_{\geq 0}$ with $t_0 \leq t$, we denote by $z_{t_0:t}$ the sequence $\{z_{t_0}, z_{t_0+1}, \dots, z_t\}$. With a slight abuse of notation, we write $z_{t_0:t} \in \mathcal{Z}$ to mean that each element of the sequence $z_{t_0:t}$ belongs to the set \mathcal{Z} .

This notation allows us to re-write (4) as

$$J_t(x_{t-L}, u_{t-L:t+T-1}, d_{t-L:t+T-1}, y_{t-L:t}) := \sum_{s=t}^{t+T-1} c_s(x_s, u_s, d_s) + q_{t+T}(x_{t+T}) - \sum_{s=t-L}^t \eta_s(y_s - g_s(x_s)) - \sum_{s=t-L}^{t+T-1} \rho_s(d_s), \quad (5)$$

which emphasizes the dependence of (5) on the unknown initial state x_{t-L} , the unknown disturbance input sequence $d_{t-L:t+T-1}$, the measured output sequence $y_{t-L:t}$, and the control input sequence $u_{t-L:t+T-1}$. Regarding the latter, one should note that $u_{t-L:t+T-1}$ is composed of two distinct sequences: the (known) past inputs $u_{t-L:t-1}$ that have already been applied and the future inputs $u_{t:t+T-1}$ that still need to be selected.

At a given time $t \in \mathbb{Z}_{\geq L}$, we do not know the value of the variables x_{t-L} and $d_{t-L:t+T-1}$ on which the value of the criterion (5) depends, so we optimize this criterion under worst-case assumptions on these variables, leading to the following min-max optimization

$$\min_{\hat{u}_{t:t+T-1}|t \in \mathcal{U}} \max_{\substack{\hat{x}_{t-L}|t \in \mathcal{X}, \\ \hat{d}_{t-L:t+T-1}|t \in \mathcal{D}, \\ \hat{n}_{t-L:t}|t \in \mathcal{N}}} J_t(\hat{x}_{t-L}|t, u_{t-L:t-1}, \hat{u}_{t:t+T-1}|t, \hat{d}_{t-L:t+T-1}|t, y_{t-L:t}), \quad (6)$$

where the arguments $u_{t-L:t-1}, \hat{u}_{t:t+T-1}|t$ to the function $J_t(\cdot)$ in (6) correspond to the argument $u_{t-L:t+T-1}$ in the definition of $J_t(\cdot)$ in the left-hand side of (5). When interpreting (6), one should view $\hat{u}_{t:t+T-1}|t \in \mathcal{U}$ as the optimization variables for the (outer) minimization, and $\hat{x}_{t-L}|t \in \mathcal{X}, \hat{d}_{t-L:t+T-1}|t \in \mathcal{D}$ as the optimization variables for the (inner) maximization. The variables $\hat{n}_{t-L:t}$ are not independent optimization variables as they are uniquely determined by the remaining optimization variables and the output equation:

$$\hat{n}_s|t = y_s - g_s(\hat{x}_s|t), \quad \forall s \in \{t-L, t-L+1, \dots, t\}.$$

Consequently, the condition $\hat{n}_{t-L:t}|t \in \mathcal{N}$ can simply be regarded as a constraint on the remaining optimization variables for the (inner) maximization.

The subscript $\cdot|t$ in the optimization variables that appear in (6) emphasizes that this optimization is repeated at each time step $t \in \mathbb{Z}_{\geq 0}$. At different time steps these optimizations typically lead to different solutions which generally do not coincide with the real control input, disturbances, and noise. We can view the optimization variables $\hat{x}_{t-L}|t$ and $\hat{d}_{t-L:t+T-1}|t$ as (worst-case) estimates of the initial state and disturbances, respectively, based

on the past inputs $u_{t-L:t-1}$ and outputs $y_{t-L:t}$ available at time t .

Inspired by MPC, at each time t , we use as the control input the first element of the sequence

$$\hat{u}_{t:t+T-1|t}^* = \{\hat{u}_{t|t}^*, \hat{u}_{t+1|t}^*, \hat{u}_{t+2|t}^*, \dots, \hat{u}_{t+T-1|t}^*\} \in \mathcal{U}$$

that minimizes (6), leading to the following control law:

$$u_t = \hat{u}_{t|t}^*, \quad \forall t \geq 0. \quad (7)$$

The relationship between this combined estimation and control approach and standard forms of MPC and MHE is discussed in Copp & Hespanha (2014).

To simplify the presentation, at this point we define a shorthand notation for the optimization variables as follows: $\hat{\mathbf{u}} := \hat{u}_{t:t+T-1|t}$, $\hat{\mathbf{d}} := \hat{d}_{t-L:t+T-1|t}$, $\hat{\mathbf{x}} := \hat{x}_{t-L|t}$. We also define a shorthand notation for the following sequences of known past inputs and outputs, respectively: $\mathbf{u} := u_{t-L:t-1}$, $\mathbf{y} := y_{t-L:t}$.

This new notation, as well as removing the dependent optimization variables $\hat{n}_{t-L:t}$, allows us to re-write (6) as

$$\min_{\hat{\mathbf{u}} \in \mathcal{U}} \max_{\substack{\hat{\mathbf{x}} \in \mathcal{X}, \\ \hat{\mathbf{d}} \in \mathcal{D}}} J_t(\hat{\mathbf{x}}, \mathbf{u}, \hat{\mathbf{u}}, \hat{\mathbf{d}}, \mathbf{y}). \quad (8)$$

Moreover, we define the variables that minimize (8) as $\hat{\mathbf{u}}^* \in \mathcal{U}$ and the variables that maximize (8) as $\hat{\mathbf{d}}^* \in \mathcal{D}$ and $\hat{\mathbf{x}}^* \in \mathcal{X}$.

This new notation will be used for the remainder of the article until the Appendix where more explicit notation is required for the proofs.

3 Closed-Loop Boundedness and Tracking

In this section, we show that the control law (7) leads to boundedness of the state of the closed-loop system under appropriate assumptions, which we discuss next.

A necessary assumption for the implementation of the control law (7) is that the outer minimization in (8) leads to finite values for the optima that are achieved at specific sequences $\hat{\mathbf{u}}^* \in \mathcal{U}$, $t \in \mathbb{Z}_{\geq 0}$. However, for the stability results in this section we actually ask for the existence of a saddle-point solution to the min-max optimization in (8), which is a common requirement in game theoretical approaches to control design (Başar & Olsder, 1995):

Assumption 1 (Saddle-point) *The min-max optimization in (8) always has a saddle-point solution for which the min and max commute. Specifically, for every*

time $t \in \mathbb{Z}_{\geq 0}$, past control input sequence $u_{t-L:t-1} \in \mathcal{U}$, and past measured output sequence $y_{t-L:t} \in \mathcal{Y}$, there exists a finite scalar $J_t^ \in \mathbb{R}$, an initial condition $\hat{\mathbf{x}}^* \in \mathcal{X}$, and sequences $\hat{\mathbf{u}}^* \in \mathcal{U}$, $\hat{\mathbf{d}}^* \in \mathcal{D}$ such that*

$$\begin{aligned} J_t^* &= J_t(\hat{\mathbf{x}}^*, \mathbf{u}, \hat{\mathbf{u}}^*, \hat{\mathbf{d}}^*, \mathbf{y}) \\ &= \max_{\substack{\hat{\mathbf{x}} \in \mathcal{X}, \\ \hat{\mathbf{d}} \in \mathcal{D}}} J_t(\hat{\mathbf{x}}, \mathbf{u}, \hat{\mathbf{u}}^*, \hat{\mathbf{d}}, \mathbf{y}) \end{aligned} \quad (9a)$$

$$= \min_{\hat{\mathbf{u}} \in \mathcal{U}} J_t(\hat{\mathbf{x}}^*, \mathbf{u}, \hat{\mathbf{u}}, \hat{\mathbf{d}}^*, \mathbf{y}). \quad (9b)$$

□

In general, J_t^* depends on the past outputs and control inputs, so we could write $J_t^*(\mathbf{u}, \mathbf{y})$ to emphasize this dependence. For simplicity, however, we use J_t^* throughout the paper to denote the optimal value of the cost function $J_t(\cdot)$.

Assumption 1 presumes an appropriate form of *observability/detectability* adapted to the criterion $\sum_{s=t}^{t+T-1} c_s(x_s, u_s, d_s)$ because (9a) implies that, for every initial condition $\hat{\mathbf{x}} \in \mathcal{X}$, disturbance sequence $\hat{\mathbf{d}} \in \mathcal{D}$, and resulting state trajectory $\hat{x}_{t-L:t+T}$,

$$\begin{aligned} c_t(\hat{x}_t, \hat{u}_{t|t}^*, \hat{d}_{t|t}) &\leq \\ J_t^* &+ \sum_{s=t-L}^{t+T-1} \rho_s(\hat{d}_{s|t}) + \sum_{s=t-L}^t \eta_s(y_s - g_s(\hat{x}_s)). \end{aligned}$$

This means that we can essentially bound the size of the *current* state using past outputs and past/future input disturbances. In fact, for linear systems and quadratic costs, Assumption 1 is satisfied if the system is observable and the weights in the cost function are chosen appropriately (Copp & Hespanha, 2016b).

To establish state boundedness under the control (7) defined by the *finite-horizon* optimization criterion (5), one needs two additional assumptions regarding the system dynamics and the terminal cost $q_{t+T}(\cdot)$.

Assumption 2 (Observability) *There exists a bounded set $\mathcal{N}_{\text{pre}} \subset \mathbb{R}^{n_x}$ such that, for every time $t \in \mathbb{Z}_{\geq 0}$, every state $\hat{x}_{t-L:t} \in \mathcal{X}$, and every disturbance and noise sequence, $\hat{d}_{t-L:t} \in \mathcal{D}$ and $\hat{n}_{t-L:t} \in \mathcal{N}$, that are compatible with the applied control input u_s , $s \in \mathbb{Z}_{\geq 0}$, and the measured output y_s , $s \in \mathbb{Z}_{\geq 0}$, in the sense that*

$$\hat{x}_{s+1} = f_s(\hat{x}_s, u_s, \hat{d}_s), \quad y_s = g_s(\hat{x}_s) + \hat{n}_s, \quad (10)$$

$\forall s \in \{t-L, t-L+1, \dots, t\}$, there exists a “predecessor” state estimate $\hat{x}_{t-L-1} \in \mathcal{X}$, disturbance estimate $\hat{d}_{t-L-1} \in \mathcal{D}$, and noise estimate $\hat{n}_{t-L-1} \in \mathcal{N}_{\text{pre}}$ such that (10) also holds for time $s = t-L-1$. □

In essence, Assumption 2 requires the past horizon length L to be sufficiently large so that, by observing the system's inputs and outputs over a past time interval $\{t-L, t-L+1, \dots, t\}$, one obtains enough information about the initial condition x_{t-L} so that any estimate \hat{x}_{t-L} that is compatible with the observed input/output data is "precise". By "precise," we mean that if one were to observe one additional past input/output pair u_{t-L-1}, y_{t-L-1} just before the original interval, it would be possible to find an estimate \hat{x}_{t-L-1} for the "predecessor" state x_{t-L-1} that would be compatible with the previous estimate \hat{x}_{t-L} , that is,

$$\hat{x}_{t-L} = f_{t-L-1}(\hat{x}_{t-L-1}, u_{t-L-1}, \hat{d}_{t-L-1}).$$

This "predecessor" state estimate \hat{x}_{t-L-1} would also be compatible with the measured output at time $t-L-1$ in the sense that the output estimation error lies in the bounded set \mathcal{N}_{pre} :

$$y_{t-L-1} - g_{t-L-1}(\hat{x}_{t-L-1}) \in \mathcal{N}_{\text{pre}}. \quad (11)$$

We do not require the bounded set \mathcal{N}_{pre} to be the same as the set \mathcal{N} in which the actual noise is known to lie. In fact, the set \mathcal{N}_{pre} where the "predecessor" output error (11) should lie may have to be made larger than \mathcal{N} to make sure that Assumption 2 holds. For linear systems, it is straightforward to argue that Assumption 2 holds provided that the matrix

$$\begin{bmatrix} C \\ CA \\ \vdots \\ CA^L \end{bmatrix}$$

is full column rank and the set \mathcal{N}_{pre} is chosen sufficiently large. For nonlinear systems, computing the set \mathcal{N}_{pre} may be difficult, but fortunately we do not need to compute this set to implement the controller.

Remark 1 (Choosing length of L) *Although computing the set \mathcal{N}_{pre} is not required, how large \mathcal{N}_{pre} needs to be is essentially determined by the length of the backwards horizon L . As the length of L is increased, equation (10) provides more constraints on the estimates which leads to better estimates and, therefore, a necessarily smaller set \mathcal{N}_{pre} . In addition, as is discussed later after (17), a smaller bound on the norm of the state x may be achieved as L is increased. Therefore, larger L is generally better, but increasing L also increases the computation required to solve (8) as the number of optimization variables increases as well. Thus, a heuristic for choosing L is to make it as large as possible given available computational resources.*

Assumption 3 (ISS-control Lyapunov function)

The terminal cost $q_t(\cdot)$ is an ISS-control Lyapunov function, in the sense that, for every $t \in \mathbb{Z}_{\geq 0}$, $x \in \mathcal{X}$, there exists a control $u \in \mathcal{U}$ such that for all $d \in \mathcal{D}$

$$q_{t+1}(f_t(x, u, d)) - q_t(x) \leq -c_t(x, u, d) + \rho_t(d). \quad (12)$$

□

Assumption 3 plays the role of the common assumption in MPC that the terminal cost must be a control Lyapunov function for the closed-loop (Mayne, Rawlings, Rao & Scokaert, 2000). In the absence of the disturbance d , (12) would mean that $q_t(\cdot)$ could be viewed as a control Lyapunov function that decreases along system trajectories for an appropriate control input u (Sontag, 1999). With disturbances, $q_t(\cdot)$ needs to be viewed as an ISS-control Lyapunov function that satisfies an ISS stability condition for the disturbance input d and an appropriate control input u (Liberzon, Sontag & Wang, 2002).

Theorem 1 (Cost-to-go bound) *Suppose that Assumptions 1, 2, and 3 hold. Along any trajectory of the closed-loop system defined by the process (1) and the control law (7), we have that*

$$\begin{aligned} c_t(x_t, u_t, d_t) &\leq J_L^* + \sum_{s=0}^{t-L-1} \rho_s(\tilde{d}_s) + \sum_{s=0}^{t-L-1} \eta_s(\tilde{n}_s) \\ &+ \sum_{s=t-L}^t \eta_s(n_s) + \sum_{s=t-L}^t \rho_s(d_s), \quad \forall t \in \mathbb{Z}_{\geq L}, \end{aligned} \quad (13)$$

for appropriate sequences $\tilde{d}_{0:t-L-1} \in \mathcal{D}$, $\tilde{n}_{0:t-L-1} \in \mathcal{N}_{\text{pre}}$. □

The terms $\sum_{s=0}^{t-L-1} \eta_s(\tilde{n}_s) + \sum_{s=0}^{t-L-1} \rho_s(\tilde{d}_s)$ in the right hand side of (13) can be thought of as the *arrival cost* that appears in the MHE literature to capture the quality of the estimate at the beginning of the current estimation window (Rao et al., 2003).

The proof of Theorem 1 is given in Appendix A.1. Next we discuss the implications of Theorem 1 in terms of establishing bounds on the state of the closed-loop system, practical stability, and the ability of the closed-loop to asymptotically track desired trajectories.

3.1 State boundedness and practical stability

When we select penalty functions in the criterion (5), for which there exists a class \mathcal{K}_{∞} function $\alpha(\cdot)$ and class \mathcal{K} functions¹ $\beta(\cdot), \delta(\cdot)$ such that

¹ A function $\alpha : \mathbb{R}_{\geq 0} \rightarrow \mathbb{R}_{\geq 0}$ is said to belong to class \mathcal{K} if it is continuous, zero at zero, and strictly increasing and is said to belong to class \mathcal{K}_{∞} if it belongs to class \mathcal{K} and is unbounded.

$$c_t(x, u, d) \geq \alpha(\|x\|), \quad \eta_t(n) \leq \beta(\|n\|), \quad \rho_t(d) \leq \delta(\|d\|), \\ \forall x \in \mathbb{R}^{n_x}, u \in \mathbb{R}^{n_u}, d \in \mathbb{R}^{n_d}, n \in \mathbb{R}^{n_n},$$

we conclude from (13) that, along trajectories of the closed-loop system, the following inequality holds for all $t \in \mathbb{Z}_{\geq L}$:

$$\alpha(\|x_t\|) \leq J_L^* + \sum_{s=0}^{t-L-1} \beta(\|\tilde{n}_s\|) + \sum_{s=0}^{t-L-1} \delta(\|\tilde{d}_s\|) \\ + \sum_{s=t-L}^t \beta(\|n_s\|) + \sum_{s=t-L}^t \delta(\|d_s\|). \quad (14)$$

Formula (14) provides a bound on the state when the future noise and disturbance signals are “vanishing,” in the sense that

$$\sum_{s=t-L}^{\infty} \beta(\|n_s\|) < \infty, \quad \sum_{s=t-L}^{\infty} \delta(\|d_s\|) < \infty.$$

Theorem 1 also provides bounds on the state for non-vanishing noise and disturbances when we use exponentially time-weighted functions $c_t(\cdot)$, $\eta_t(\cdot)$, and $\rho_t(\cdot)$ that satisfy

$$c_t(x, u, d) \geq \lambda^{-t} \alpha(\|x\|), \quad (15a)$$

$$\eta_t(n) \leq \lambda^{-t} \beta(\|n\|), \quad (15b)$$

$$\rho_t(d) \leq \lambda^{-t} \delta(\|d\|), \quad (15c)$$

for all $x \in \mathbb{R}^{n_x}, u \in \mathbb{R}^{n_u}, d \in \mathbb{R}^{n_d}, n \in \mathbb{R}^{n_n}$ and some $\lambda \in (0, 1)$. In this case, we conclude from (13) that for all $t \in \mathbb{Z}_{\geq L}$,

$$\alpha(\|x_t\|) \leq \lambda^t J_L^* \\ + \sum_{s=0}^{t-L-1} \lambda^{t-s} \beta(\|\tilde{n}_s\|) + \sum_{s=0}^{t-L-1} \lambda^{t-s} \delta(\|\tilde{d}_s\|) \\ + \sum_{s=t-L}^t \lambda^{t-s} \beta(\|n_s\|) + \sum_{s=t-L}^t \lambda^{t-s} \delta(\|d_s\|). \quad (16)$$

Therefore, x_t remains bounded because $n_s \in \mathcal{N}$, $\tilde{n}_s \in \mathcal{N}_{\text{pre}}$, $d_s \in \mathcal{D}$, $\tilde{d}_s \in \mathcal{D}$, and the three sets \mathcal{N} , \mathcal{N}_{pre} , and \mathcal{D} are bounded. More specifically, if the noise and disturbances are uniformly bounded such that, for all $s \geq 0$,

$$\beta(\|\tilde{n}_s\|) \leq \tilde{a}, \quad \beta(\|n_s\|) \leq a, \quad \delta(\|\tilde{d}_s\|) \leq \tilde{b}, \quad \delta(\|d_s\|) \leq b,$$

where \tilde{a} , \tilde{b} , and b are finite scalars, then an analytical upper bound can be computed for $\alpha(\|x_t\|)$, using the formula for geometric series, and is given by

$$\alpha(\|x_t\|) \leq \lambda^t J_L^* \\ + (\tilde{a} + \tilde{b}) \left(\frac{\lambda^{L+1} - \lambda^{t+1}}{1 - \lambda} \right) + (a + b) \left(\frac{1 - \lambda^{L+1}}{1 - \lambda} \right). \quad (17)$$

Moreover, the terms in the right-hand-side of (17) that depend on \tilde{n} and \tilde{d} can be made arbitrarily small by increasing L . The first term in the right-hand-side of (17) may initially be large as L is increased, but it exponentially decays to a small value as $t \rightarrow \infty$. Finally, if the true noise and disturbances vanish asymptotically, then the terms in the right-hand-side of (16) that depend on n_s and d_s converge to zero as $t \rightarrow \infty$. Therefore, $\|x_t\|$ converges to a small value as $t \rightarrow \infty$ when the true noise and disturbances vanish asymptotically and the backwards horizon is chosen arbitrarily large. We have proved the following:

Corollary 1 *Suppose that Assumptions 1, 2, and 3 hold and also that (15) holds for a class \mathcal{K}_{∞} function $\alpha(\cdot)$, class \mathcal{K} functions $\beta(\cdot)$, $\delta(\cdot)$, and $\lambda \in (0, 1)$. Then, for every initial condition x_0 , uniformly bounded measurement noise sequence $n_{0:t}$, and uniformly bounded disturbance sequence $d_{0:t}$, the state x_t remains uniformly bounded along the trajectories of the process (1) with control (7) defined by the finite-horizon optimization (6). Moreover, when d_t and n_t converge to zero as $t \rightarrow \infty$, the backwards horizon L can be chosen sufficiently large to ensure that the state x_t converges to an arbitrarily small value as $t \rightarrow \infty$. \square*

Remark 2 (Time-weighted criteria) *The exponentially time-weighted functions (15) typically arise from a criterion of the form*

$$\sum_{s=t}^{t+T-1} \lambda^{-s} c(x_s, u_s, d_s) + q_{t+T}(x_{t+T}) \\ - \sum_{s=t-L}^t \lambda^{-s} \eta(n_s) - \sum_{s=t-L}^{t+T-1} \lambda^{-s} \rho(d_s)$$

that weight the future more than the past. In this case, (15) holds for functions $\alpha(\cdot)$, $\beta(\cdot)$, and $\delta(\cdot)$ such that $c(x, u, d) \geq \alpha(\|x\|)$, $\eta(n) \leq \beta(\|n\|)$, and $\rho(d) \leq \delta(\|d\|)$, $\forall x, u, d, n$. \square

3.2 Reference tracking

When the control objective is for the state x_t to follow a given trajectory z_t , the optimization criterion can be selected of the form

$$\sum_{s=t}^{t+T-1} \lambda^{-s} c(x_s - z_s, u_s, d_s) + q_{t+T}(x_{t+T} - z_{t+T}) \\ - \sum_{s=t-L}^t \lambda^{-s} \eta(n_s) - \sum_{s=t-L}^{t+T-1} \lambda^{-s} \rho(d_s),$$

with $c(x - z, u, d) \geq \alpha(\|x - z\|)$, $\forall x, u, d$ for some class \mathcal{K}_{∞} function α and $\lambda \in (0, 1)$. In this case, we conclude from (13) that, for all $t \in \mathbb{Z}_{\geq L}$,

$$\begin{aligned} \alpha(\|x_t - z_t\|) &\leq \lambda^t J_L^* \\ &+ \sum_{s=0}^{t-L-1} \lambda^{t-s} \eta(\tilde{n}_s) + \sum_{s=0}^{t-L-1} \lambda^{t-s} \rho(\tilde{d}_s) \\ &+ \sum_{s=t-L}^t \lambda^{t-s} \eta(n_s) + \sum_{s=t-L}^t \lambda^{t-s} \rho(d_s), \end{aligned}$$

which allows us to conclude, from Corollary 1, that x_t converges arbitrarily close to z_t as $t \rightarrow \infty$ when both n_t and d_t are vanishing sequences and L is chosen sufficiently large. Similarly, if these noise and disturbance sequences are “ultimately small”, the tracking error $x_t - z_t$ will converge to a small value.

4 Computation of Control by Solving a Pair of Coupled Optimizations

To implement the control law (7) we need to find the control sequence $\hat{\mathbf{u}}^* \in \mathcal{U}$ that achieves the outer minimization in (8). In view of Assumption 1, the desired control sequence must be part of the saddle-point defined by (9a)–(9b). It turns out that it is more convenient to use the following equivalent characterization of the saddle point:

$$-J_t^* = \min_{\substack{\hat{\mathbf{x}} \in \mathcal{X}, \\ \hat{\mathbf{d}} \in \mathcal{D}}} -J_t(\hat{\mathbf{x}}, \mathbf{u}, \hat{\mathbf{u}}^*, \hat{\mathbf{d}}, \mathbf{y}) \quad (18a)$$

$$J_t^* = \min_{\hat{\mathbf{u}} \in \mathcal{U}} J_t(\hat{\mathbf{x}}^*, \mathbf{u}, \hat{\mathbf{u}}, \hat{\mathbf{d}}^*, \mathbf{y}) \quad (18b)$$

where we introduced the “-” sign in (18a) simply to obtain two minimizations, instead of a maximization and one minimization, which will somewhat simplify the presentation.

Since the process dynamics (1) has a unique solution for any given initial condition, control input, and unmeasured disturbance, the coupled optimizations in (18) can be re-written as

$$\begin{aligned} -J_t^* &= \min_{(\hat{\mathbf{d}}, \bar{\mathbf{x}}) \in \bar{\mathcal{D}}[\mathbf{u}, \hat{\mathbf{u}}^*]} \\ &- \sum_{s=t}^{t+T-1} c_s(\bar{x}_s, \hat{u}_s^*, \hat{d}_s) - q_{t+T}(\bar{x}_{t+T}) \\ &+ \sum_{s=t-L}^t \eta_s(y_s - g_s(\bar{x}_s)) + \sum_{s=t-L}^{t+T-1} \rho_s(\hat{d}_s), \quad (19a) \end{aligned}$$

$$\begin{aligned} J_t^* &= \min_{(\hat{\mathbf{u}}, \bar{\mathbf{x}}) \in \bar{\mathcal{U}}[\bar{x}_{t-L}^*, \hat{\mathbf{d}}^*]} \\ &\sum_{s=t}^{t+T-1} c_s(\tilde{x}_s, \hat{u}_s, \hat{d}_s^*) + q_{t+T}(\tilde{x}_{t+T}) \\ &- \sum_{s=t-L}^t \eta_s(y_s - g_s(\tilde{x}_s)) - \sum_{s=t-L}^{t+T-1} \rho_s(\hat{d}_s^*) \quad (19b) \end{aligned}$$

where $\bar{\mathbf{x}} := \bar{x}_{t-L:t+T|t}$, $\tilde{\mathbf{x}} := \tilde{x}_{t-L+1:t+T|t}$, $\tilde{x}_{t-L} = \bar{x}_{t-L}^*$, and

$$\begin{aligned} \bar{\mathcal{D}}[\mathbf{u}, \hat{\mathbf{u}}^*] &:= \left\{ (\hat{\mathbf{d}}, \bar{\mathbf{x}}) : \hat{\mathbf{d}} \in \mathcal{D}, \bar{\mathbf{x}} \in \mathcal{X}, \right. \\ &\bar{x}_{s+1} = f_s(\bar{x}_s, u_s, \hat{d}_s), \forall s \in \{t-L, \dots, t-1\}, \\ &\left. \bar{x}_{s+1} = f_s(\bar{x}_s, \hat{u}_s^*, \hat{d}_s), \forall s \in \{t, \dots, t+T-1\} \right\} \quad (20a) \end{aligned}$$

$$\begin{aligned} \bar{\mathcal{U}}[\bar{x}_{t-L}^*, \hat{\mathbf{d}}^*] &:= \left\{ (\hat{\mathbf{u}}, \bar{\mathbf{x}}) : \hat{\mathbf{u}} \in \mathcal{U}, \bar{\mathbf{x}} \in \mathcal{X}, \right. \\ &\tilde{x}_{t-L+1} = f_{t-L}(\bar{x}_{t-L}^*, u_{t-L}, \hat{d}_{t-L}^*), \\ &\tilde{x}_{s+1} = f_s(\tilde{x}_s, u_s, \hat{d}_s^*), \forall s \in \{t-L+1, \dots, t-1\}, \\ &\left. \tilde{x}_{s+1} = f_s(\tilde{x}_s, \hat{u}_s, \hat{d}_s^*), \forall s \in \{t, \dots, t+T-1\} \right\}. \quad (20b) \end{aligned}$$

To obtain the optimizations in (19), we introduce the values of the state from time $t-L+1$ to time $t+T$, that are constrained by the system dynamics, as additional optimization variables in each of the optimizations in (18). This is a common technique used when solving optimization problems numerically (Betts, 2010). While this introduces additional optimization variables, it avoids the need to explicitly evaluate the solution to (1) that appears in the original optimizations (18) and that can be numerically poorly conditioned, e.g., for systems with unstable dynamics.

While the numerical method discussed in the next section can be used to solve either (18) or (19), our numerical example uses the latter because it generally leads to simpler optimization problems. Therefore we focus our discussion on that approach.

5 Interior-Point Method for Minimax Problems

The coupled optimizations in (18) or (19) can be viewed as a special case of the following more general problem: Find a pair $(u^*, d^*) \in \mathcal{U}[d^*] \times \mathcal{D}[u^*]$ that simultaneously solves the two coupled optimizations

$$f(u^*, d^*) = \min_{u \in \mathcal{U}[d^*]} f(u, d^*), \quad (21a)$$

$$g(u^*, d^*) = \min_{d \in \mathcal{D}[u^*]} g(u^*, d), \quad (21b)$$

with

$$\mathcal{U}[d] := \{u \in \mathbb{R}^{N_u} : F_u(u, d) \geq 0, G_u(u, d) = 0\}, \quad (22a)$$

$$\mathcal{D}[u] := \{d \in \mathbb{R}^{N_d} : F_d(u, d) \geq 0, G_d(u, d) = 0\}, \quad (22b)$$

for given functions $f : \mathbb{R}^{N_u} \times \mathbb{R}^{N_d} \in \mathbb{R}$, $g : \mathbb{R}^{N_u} \times \mathbb{R}^{N_d} \in \mathbb{R}$, $F_u : \mathbb{R}^{N_u} \times \mathbb{R}^{N_d} \rightarrow \mathbb{R}^{M_u}$, $F_d : \mathbb{R}^{N_u} \times \mathbb{R}^{N_d} \rightarrow \mathbb{R}^{M_d}$, $G_u : \mathbb{R}^{N_u} \times \mathbb{R}^{N_d} \rightarrow \mathbb{R}^{K_u}$, $G_d : \mathbb{R}^{N_u} \times \mathbb{R}^{N_d} \rightarrow \mathbb{R}^{K_d}$. To map (19) to (21), one would associate the vectors $u \in \mathbb{R}^{N_u}$ and $d \in \mathbb{R}^{N_d}$ in (21) with the sequences in

the sets $\bar{\mathcal{D}}[\cdot]$ and $\bar{\mathcal{U}}[\cdot]$ in (20). In this case, the equality constraints in (22) would typically correspond to the system dynamics, and the inequality constraints in (22) would enforce that the state, control, and disturbance signals belong, respectively, to the sets \mathcal{X} , \mathcal{U} , and \mathcal{D} introduced below (1).

Remark 3 *The optimization in (21) is more general than the one in (19) in that the function being minimized in (19a) is the symmetric of the function being minimized in (19b), whereas in (21), f and g need not be the symmetric of each other. While this generalization does not appear to be particularly useful for our output-feedback MPC application, all the results that follow do apply to general functions f and g and can be useful for other applications.*

The following duality-like result provides the motivation for a primal-dual-like method to solve the coupled minimizations in (21). It provides a set of conditions, involving an unconstrained optimization, that provide an approximation to the solution of (21).

Lemma 1 (Approximate equilibrium) *Suppose that we have found primal variables $\hat{u} \in \mathbb{R}^{N_u}$, $\hat{d} \in \mathbb{R}^{N_d}$ and dual variables $\hat{\lambda}_{fu} \in \mathbb{R}^{M_u}$, $\hat{\lambda}_{gd} \in \mathbb{R}^{M_d}$, $\hat{\nu}_{fu} \in \mathbb{R}^{K_u}$, $\hat{\nu}_{gd} \in \mathbb{R}^{K_d}$ that simultaneously satisfy all of the following conditions²*

$$G_u(\hat{u}, \hat{d}) = 0, \quad G_d(\hat{u}, \hat{d}) = 0, \quad (23a)$$

$$\hat{\lambda}_{fu} \geq 0, \quad \hat{\lambda}_{gd} \geq 0, \quad F_u(\hat{u}, \hat{d}) \geq 0, \quad F_d(\hat{u}, \hat{d}) \geq 0, \quad (23b)$$

$$L_f(\hat{u}, \hat{d}, \hat{\lambda}_{fu}, \hat{\nu}_{fu}) = \min_{u \in \mathbb{R}^{N_u}} L_f(u, \hat{d}, \hat{\lambda}_{fu}, \hat{\nu}_{fu}), \quad (23c)$$

$$L_g(\hat{u}, \hat{d}, \hat{\lambda}_{gd}, \hat{\nu}_{gd}) = \min_{d \in \mathbb{R}^{N_d}} L_g(\hat{u}, d, \hat{\lambda}_{gd}, \hat{\nu}_{gd})$$

where, for all u , d , λ , and ν ,

$$L_f(u, d, \lambda_{fu}, \nu_{fu}) := f(u, d) - \lambda_{fu} F_u(u, d) + \nu_{fu} G_u(u, d),$$

$$L_g(u, d, \lambda_{gd}, \nu_{gd}) := g(u, d) - \lambda_{gd} F_d(u, d) + \nu_{gd} G_d(u, d).$$

Then (\hat{u}, \hat{d}) approximately satisfy (21) in the sense that

$$f(\hat{u}, \hat{d}) \leq \epsilon_f + \min_{u \in \mathcal{U}[\hat{d}]} f(u, \hat{d}), \quad (24a)$$

$$g(\hat{u}, \hat{d}) \leq \epsilon_g + \min_{d \in \mathcal{D}[\hat{u}]} g(\hat{u}, d), \quad (24b)$$

with

$$\epsilon_f := \hat{\lambda}_{fu} F_u(\hat{u}, \hat{d}), \quad \epsilon_g := \hat{\lambda}_{gd} F_d(\hat{u}, \hat{d}). \quad (25)$$

□

² Given a vector $x \in \mathbb{R}^n$ and a scalar $a \in \mathbb{R}$, we denote by $x \geq a$ the proposition that every entry of x is greater than or equal to a .

The proof of this Lemma can be found in Appendix A.2.

5.1 Interior-point primal-dual equilibria algorithm

The proposed method consists of using Newton iterations to solve a system of nonlinear equations on the primal variables $\hat{u} \in \mathbb{R}^{N_u}$, $\hat{d} \in \mathbb{R}^{N_d}$ and dual variables $\hat{\lambda}_{fu} \in \mathbb{R}^{M_u}$, $\hat{\lambda}_{gd} \in \mathbb{R}^{M_d}$, $\hat{\nu}_{fu} \in \mathbb{R}^{K_u}$, $\hat{\nu}_{gd} \in \mathbb{R}^{K_d}$ introduced in Lemma 1. Throughout this section, we ask that L_f and L_g are continuously differentiable with respect to u and d , respectively (see Remark 5 below). The specific system of equations consists of:

- (1) the first-order optimality conditions for the unconstrained minimizations in (23c)³:

$$\nabla_u L_f(\hat{u}, \hat{d}, \hat{\lambda}_{fu}, \hat{\nu}_{fu}) = \mathbf{0}_{N_u}, \quad (26a)$$

$$\nabla_d L_g(\hat{u}, \hat{d}, \hat{\lambda}_{gd}, \hat{\nu}_{gd}) = \mathbf{0}_{N_d}; \quad (26b)$$

- (2) the equality conditions (23a); and

- (3) the equations⁴

$$F_u(\hat{u}, \hat{d}) \odot \hat{\lambda}_{fu} = \mu \mathbf{1}_{M_u}, \quad (27a)$$

$$F_d(\hat{u}, \hat{d}) \odot \hat{\lambda}_{gd} = \mu \mathbf{1}_{M_d}, \quad (27b)$$

for some $\mu > 0$, which leads to

$$\epsilon_f = M_u \mu, \quad \epsilon_g = M_d \mu.$$

Since our goal is to find primal variables \hat{u}, \hat{d} for which (24) holds with $\epsilon_f = \epsilon_g = 0$, we shall make the variable μ converge to zero as the Newton iterations progress. This is done in the context of an interior-point method, meaning that all variables will be initialized so that the inequality constraints (23b) hold, and the progression along the Newton direction at each iteration will be selected so that these constraints are never violated.

The specific steps of the algorithm that follows are based on the primal-dual interior-point method for a single optimization, as described in Vandenberghe (2010). To describe this algorithm, we define

$$z := [\hat{u} \ \hat{d}]', \quad \lambda := [\hat{\lambda}_{fu} \ \hat{\lambda}_{gd}]', \quad \nu := [\hat{\nu}_{fu} \ \hat{\nu}_{gd}]',$$

$$G(z) := \begin{bmatrix} G_u(\hat{u}, \hat{d}) \\ G_d(\hat{u}, \hat{d}) \end{bmatrix}, \quad F(z) := \begin{bmatrix} F_u(\hat{u}, \hat{d}) \\ F_d(\hat{u}, \hat{d}) \end{bmatrix},$$

which allows us to re-write (26), (23a), and (27) as

$$\nabla_u L_f(z, \lambda, \nu) = \mathbf{0}_{N_u}, \quad \nabla_d L_g(z, \lambda, \nu) = \mathbf{0}_{N_d}, \quad (28a)$$

³ Given an integer M , we denote by $\mathbf{0}_M$ and by $\mathbf{1}_M$ the M -vectors with all entries equal to 0 and 1, respectively.

⁴ Given two vectors $x, y \in \mathbb{R}^n$ we denote by $x \odot y \in \mathbb{R}^n$ and by $x \oslash y \in \mathbb{R}^n$ the entry-wise product and division of the two vectors, respectively.

$$G(z) = \mathbf{0}_{K_u+K_d}, \quad \lambda \odot F(z) = \mu \mathbf{1}_{M_u+M_d}, \quad (28b)$$

and (23b) as

$$\lambda \geq \mathbf{0}_{M_u+M_d}, \quad F(z) \geq \mathbf{0}_{M_u+M_d}. \quad (28c)$$

5.1.1 Primal-dual optimization algorithm:

Step 1. Start with estimates z_0, λ_0, ν_0 that satisfy the inequalities $\lambda_0 \geq 0$, $F(z_0) \geq 0$ in (28c), and set $\mu_0 = 1$ and $k = 0$. It is often a good idea to start with a value for z_0 that satisfies the equality constraint $G(z_0) = 0$, and $\lambda_0 = \mu_0 \mathbf{1}_{M_u+M_d} \oslash F(z_0)$, which guarantees that we initially have $\lambda_0 \odot F(z_0) = \mu_0 \mathbf{1}_{M_u+M_d}$.

Step 2. Linearize the equations in (28a) around a current estimate z_k, λ_k, ν_k , and μ_k leading to

$$\begin{aligned} & \begin{bmatrix} \nabla_{uz} L_f(\cdot) & \nabla_{uv} L_f(\cdot) & \nabla_{u\lambda} L_f(\cdot) \\ \nabla_{dz} L_g(\cdot) & \nabla_{d\nu} L_g(\cdot) & \nabla_{d\lambda} L_g(\cdot) \\ \nabla_z G(z_k) & 0 & 0 \\ \text{diag}(\lambda_k) \nabla_z F(z_k) & 0 & \text{diag}[F(z_k)] \end{bmatrix} \begin{bmatrix} \Delta z \\ \Delta \nu \\ \Delta \lambda \end{bmatrix} \\ & = - \begin{bmatrix} \nabla_u L_f(z_k, \lambda_k, \nu_k) \\ \nabla_d L_g(z_k, \lambda_k, \nu_k) \\ G(z_k) \\ F(z_k) \odot \lambda_k - \mu_k \mathbf{1} \end{bmatrix}, \quad (29) \end{aligned}$$

where $L_f(z_k, \lambda_k, \nu_k)$ and $L_g(z_k, \lambda_k, \nu_k)$ have been compactly written as $L_f(\cdot)$ and $L_g(\cdot)$, respectively.

Step 3. Find the search direction $[\Delta z'_s \ \Delta \nu'_s \ \Delta \lambda'_s]'$ by solving (29).

Step 4. Update the estimates along the search direction so that the inequalities in (28c) hold strictly:

$$\begin{aligned} z_{k+1} &= z_k + \alpha_s \Delta z_s, \\ \nu_{k+1} &= \nu_k + \alpha_s \Delta \nu_s, \\ \lambda_{k+1} &= \lambda_k + \alpha_s \Delta \lambda_s \end{aligned}$$

where

$$\alpha_s := \min\{\alpha_{\text{primal}}, \alpha_{\text{dual}}\},$$

and

$$\begin{aligned} \alpha_{\text{primal}} &:= \max\{\alpha \in [0, 1] : F(z_k + \frac{\alpha}{.99} \Delta z_s) \geq 0\}, \\ \alpha_{\text{dual}} &:= \max\{\alpha \in [0, 1] : \lambda_k + \frac{\alpha}{.99} \Delta \lambda_s \geq 0\}. \end{aligned}$$

Also update μ_k according to

$$\mu_{k+1} = \xi \mu_k,$$

where the positive scalar ξ is chosen such that $\xi < 1$.

Step 5. Repeat from Step 2 with an incremented value for k until

$$\|\nabla_u L_f(z_k, \lambda_k, \nu_k)\| \leq \epsilon_u, \quad \|\nabla_d L_g(z_k, \lambda_k, \nu_k)\| \leq \epsilon_d, \quad (30a)$$

$$\|G(z_k)\| \leq \epsilon_G, \quad \lambda'_k F(z_k) \leq \epsilon_{\text{gap}}, \quad (30b)$$

for sufficiently small tolerances $\epsilon_u, \epsilon_d, \epsilon_G, \epsilon_{\text{gap}}$. \square

Remark 4 For additional computational efficiency, an affine scaling step may be included after Step 2 in the algorithm above. In this case, an affine scaling direction $[\Delta z'_a \ \Delta \nu'_a \ \Delta \lambda'_a]'$ is found by solving (29) for $\mu_k = 0$.

Then scalings are selected so that the inequalities in (28c) are not violated along the affine scaling direction:

$$\alpha_a := \min\{\alpha_{\text{primal}}, \alpha_{\text{dual}}\},$$

where

$$\begin{aligned} \alpha_{\text{primal}} &:= \max\{\alpha \in [0, 1] : F(z_k + \alpha \Delta z_a) \geq 0\}, \\ \alpha_{\text{dual}} &:= \max\{\alpha \in [0, 1] : \lambda_k + \alpha \Delta \lambda_a \geq 0\}. \end{aligned}$$

Define the following estimate for the “quality” of the affine scaling direction

$$\sigma := \left(\frac{F(z_k + \alpha_{\text{primal}} \Delta z_a)' (\lambda_k + \alpha_{\text{dual}} \Delta \lambda_a)}{F(z_k)' \lambda_k} \right)^\delta,$$

where δ is a parameter typically selected equal to 2 or 3. Note that the numerator $F(z_k + \alpha_{\text{primal}} \Delta z_a)' (\lambda_k + \alpha_{\text{dual}} \Delta \lambda_a)$ is the value one would obtain for $\lambda' F(z)$ by moving purely along the affine scaling directions. A small value for σ thus indicates that a significant reduction in μ_k is possible.

Finally, the new search direction $[\Delta z'_s \ \Delta \nu'_s \ \Delta \lambda'_s]'$ is found by solving (29) for $\mu_k = \sigma \frac{F(z_k) \odot \lambda_k}{M_u + M_d}$, and the algorithm continues as above with Step 4. \square

When the functions L_f and L_g that appear in the unconstrained minimizations in (23c) have a single stationary point that corresponds to their global minimum, termination of the Algorithm 5.1.1 guarantees that the assumptions of Lemma 1 hold [up to the tolerances in (30)], and we obtain the desired solution to (21).

The desired uniqueness of the stationary point holds, e.g., when the function $f(u, d)$ is convex in u , $g(u, d)$ is convex in d , $F_u(u, d)$ is concave in u , $F_d(u, d)$ is concave in d , and $G_u(u, d)$ is linear in u , and $G_d(u, d)$ is linear in d . However, in practice the Algorithm 5.1.1 can find solutions to (21) even when these convexity assumptions do not hold. For problems for which one cannot be sure

whether the Algorithm 5.1.1 terminated at a global minimum of the unconstrained problem, one may run several instances of the algorithm with random initial conditions. Consistent results for the optimizations across multiple initializations will provide an indication that a global minimum has been found.

Remark 5 (Smoothness) *Algorithm 5.1.1 requires all the functions f, g, F_u, F_d, G_u, G_d to be twice differentiable for the computation of the matrices that appear in (29). However, this does not preclude the use of this algorithm in many problems where these functions are not differentiable because it is often possible to re-formulate non-smooth optimizations into smooth ones by appropriate transformations that often introduce additional optimization variables. Common examples of these transformations include the minimization of criteria involving ℓ_p norms, such as the “non-differentiable ℓ_1 optimization”*

$$\min \{ \|A_{m \times n}x - b\|_{\ell_1} + \dots : x \in \mathbb{R}^n, \dots \}$$

which is equivalent to the following constrained smooth optimization

$$\min \{ v' \mathbf{1}_m + \dots : x \in \mathbb{R}^n, v \in \mathbb{R}^m, -v \leq Ax - b \leq v, \dots \};$$

and the “non-differentiable ℓ_2 optimization”

$$\min \{ \|A_{m \times n}x - b\|_{\ell_2} + \dots : x \in \mathbb{R}^n, \dots \}$$

which is equivalent to

$$\min \{ v + \dots : x \in \mathbb{R}^n, v \geq 0, v^2 \geq (Ax - b)'(Ax - b), \dots \}.$$

More examples of such transformations can be found, e.g., in Grant & Boyd (2008); Nesterov (2005). \square

6 Numerical Example

In this Section we discuss a numerical example using the problem framework introduced in Section 2 and find solutions via simulation using the interior-point method described in Section 5.

Example 1 (Nonlinear Pursuit-Evasion) *In this example a two-player pursuit-evasion game is considered where the pursuer is modeled as a nonholonomic unicycle-type vehicle, and the evader is modeled as a single-integrator. The measured output is the positions of the pursuer and evader. The orientation of the pursuer is not measured. The models can be written in discrete-time as follows:*

$$\begin{aligned} \text{Pursuer :} \quad & p_{t+1}^1 = p_t^1 + v \cos(\theta_t), \\ & p_{t+1}^2 = p_t^2 + v \sin(\theta_t), \\ & \theta_{t+1} = \theta_t + u_t, \end{aligned} \quad (31a)$$

$$\begin{aligned} \text{Evader :} \quad & z_{t+1}^1 = z_t^1 + d_t^1, \\ & z_{t+1}^2 = z_t^2 + d_t^2, \end{aligned} \quad (31b)$$

$$\text{Output :} \quad y_t = [p_t' \quad z_t']' + n_t. \quad (31c)$$

The positions of the pursuer and the evader at time t are denoted by $p_t = [p_t^1 \ p_t^2]' \in \mathbb{R}^2$ and $z_t = [z_t^1 \ z_t^2]' \in \mathbb{R}^2$, respectively, and the orientation of the pursuer at time t is denoted by $\theta_t \in [-\pi, \pi]$. The full state for this example at time t can then be defined as $x_t = [p_t' \ \theta_t \ z_t']' \in \mathbb{R}^2 \times [-\pi, \pi] \times \mathbb{R}^2$. The inputs for the pursuer and evader at time t are denoted by $u_t \in \mathcal{U}$ and $d_t = [d_t^1 \ d_t^2]' \in \mathcal{D}$, respectively, where the constraint sets are defined as $\mathcal{U} := \{u_t \in \mathbb{R} : |u_t| \leq u_{max}\}$ and $\mathcal{D} := \{d_t \in \mathbb{R}^2 : \|d_t\|_{\infty} \leq d_{max}\}$. The measurement noise is denoted by $n_t \in \mathbb{R}^4$. In this example, the noise is unconstrained, i.e., $\mathcal{N} = \mathbb{R}^4$; however, the weight λ_n in the cost function (32) below essentially penalizes large noise.

The evader’s goal is to make the distance between its position z_t and the position of the pursuer p_t as large as possible, so the evader wants to maximize the value of $\|z_t - p_t\|_2$. The pursuer’s goal is to do the opposite, namely, minimize the value of $\|z_t - p_t\|_2$. The pursuer and evader try to achieve these goals by choosing appropriate values for u_t and d_t , respectively. In the context of the problem described in Section 2, we regard the input for the pursuer as the control signal and the input to the evader as a disturbance. This motivates considering a cost function of the form

$$\begin{aligned} J_t(\cdot) = & \sum_{s=t}^{t+T-1} \|z_s - p_s\|_2^2 + \lambda_u \sum_{s=t}^{t+T-1} \|u_s\|_2^2 \\ & - \lambda_n \sum_{s=t-L}^t \|n_s\|_2^2 - \lambda_d \sum_{s=t-L}^{t+T-1} \|d_s\|_2^2, \end{aligned} \quad (32)$$

where λ_u , λ_n , and λ_d are positive weighting constants.

Figures 1 and 2 show simulation results from solving the optimization

$$\min_{u_{t:t+T-1} \in \mathcal{U}} \max_{\substack{x_{t-L} \in \mathcal{X}, \\ d_{t-L:t+T-1} \in \mathcal{D}}} J_t(\cdot) \quad (33)$$

at each time step t , where $J_t(\cdot)$ is the cost function given in (32), and the optimization is solved using Algorithm 5.1.1. For this nonlinear example, we can verify numerically that (9) in Assumption 1 holds along closed trajectories by comparing the values of the two coupled optimizations given in (19a) and (19b).

In this simulation, the parameters for the model (31) and the cost function (32) are chosen as $L = 8$, $T = 12$, $v = 0.1$, $u_{max} = 0.5$, $d_{max} = 0.06$, $\lambda_u = 8$, $\lambda_d = 100$,

and $\lambda_n = 1000$. The output measurements are subjected to normally distributed random noise $n_t \sim \mathcal{N}(0, 0.005^2)$.

Figure 1 shows the estimates of the pursuer’s and evader’s positions computed by solving the optimization (33) at every time t . The initial state of the pursuer is $[p_0^1 \theta_0]^T = [0 \ 0 \ 0]^T$, and the initial state of the evader is $z_0 = [0.5 \ 0.5]^T$. The simulation is initialized with zero input for the pursuer (i.e. $u_t = 0$) for the first $L = 8$ time steps after which time the optimization (33) is solved at every time step t , and the optimal input u_t^* is applied for the rest of the simulation. The evader applies an input of $d_t = [0.05 \ 0]^T$ until time $t = 55$ after which time the optimal computed evader’s input d_t^* is applied for every successive time step t . The inputs that are applied are shown in Figure 2. We see that several times throughout the simulation the input constraints for both the pursuer and evader are active.

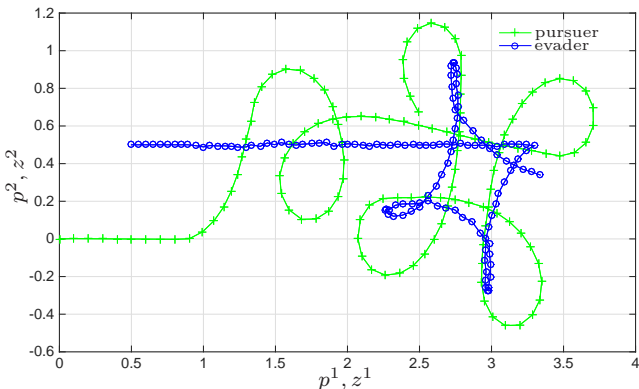


Fig. 1. Trajectories of the pursuer and evader from Example 1.

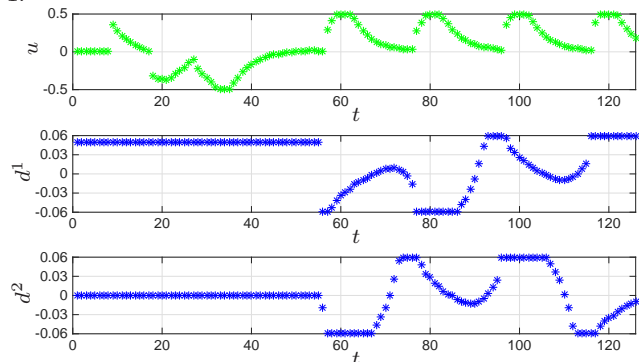


Fig. 2. Inputs for the pursuer and evader from Example 1.

Because the maximum speed of the evader ($d_{max} = 0.06$) is less than the speed of the pursuer ($v = 0.1$), the pursuer is always able to catch up to the evader, but the evader takes advantage of its more agile (integrator) dynamics by making sharp turns and forcing the unicycle-type pursuer to make loops at its maximum turning rate.

This simulation was performed on a laptop with an Intel[®] Core[™] i7 Processor and used Algorithm 5.1.1 implemented in C code to compute solutions at each time step.

The optimization involved 157 optimization variables, 100 equality constraints, and 104 inequality constraints, and the average time to compute the solution at each time step was 1.5 ms. The minimum and maximum computation times were 0.46 ms, and 4.3 ms, respectively. Therefore, solutions can be computed extremely efficiently even for this nonlinear and nonconvex example. \triangle

7 Conclusions and Future Work

We presented an output-feedback approach to nonlinear MPC with MHE. Solutions were found by combining control and state estimation into a single min-max optimization. We showed in Theorem 1 and Corollary 1 that the state of the system remains bounded, and a bound on the tracking error for reference tracking problems can be established. These results required that a saddle-point equilibrium exists (which presumes standard observability/detectability) for the min-max optimization problem, that an ISS-control Lyapunov function is included as a terminal cost, and that the backwards horizon L is sufficiently large in order to find a “predecessor” state estimate that is consistent with the dynamics.

Next we presented a primal-dual interior-point algorithm that can be used to solve general nonlinear min-max optimization problems. We validated this algorithm by showing simulation results for a nonlinear and non-convex example. Further examples can be found in the technical report by Copp & Hespanha (2015) and the book chapter by Copp & Hespanha (2016a).

Future work may involve a convergence analysis of Algorithm 5.1.1. The development of similar algorithms to solve these types of optimization problems and trade offs between methods should be investigated. For example, a Barrier interior-point algorithm could be developed which may be more robust than the primal-dual algorithm for non-convex poorly conditioned problems.

A Proofs

A.1 Proof of Theorem 1

Before proving Theorem 1, we introduce a key technical lemma that establishes a monotonicity-like property of the sequence $\{J_t^* : t \in \mathbb{Z}_{\geq 0}\}$ computed along solutions to the closed loop.

Lemma 2 Suppose that Assumptions 1, 2, and 3 hold. Along any trajectory of the closed-loop system defined by the process (1) and the control law (7), the sequence $\{J_t^* : t \in \mathbb{Z}_{\geq 0}\}$, whose existence is guaranteed by Assumption 1, satisfies

$$J_{t+1}^* - J_t^* \leq \eta_{t-L}(\tilde{n}_{t-L}) + \rho_{t-L}(\tilde{d}_{t-L}), \quad \forall t \in \mathbb{Z}_{\geq L} \quad (\text{A.1})$$

for appropriate sequences $\tilde{d}_{0:t-L-1} \in \mathcal{D}$, $\tilde{n}_{0:t-L-1} \in \mathcal{N}_{\text{pre}}$. \square

The following notation will be used in the remainder of the proof to denote the solution to process (1): given a control input sequence $u_{t-L:t-1}$ and a disturbance input sequence $d_{t-L:t-1}$, we denote by

$$\varphi(t; t-L, x_{t-L}, u_{t-L:t-1}, d_{t-L:t-1})$$

the state x_t of the system (1) at time t for the given inputs and initial condition x_{t-L} .

Proof of Lemma 2. From (9b) in Assumption 1 at time $t+1$, we conclude that there exists an initial condition $\hat{x}_{t-L+1|t+1}^* \in \mathcal{X}$ and sequences $\hat{d}_{t-L+1:t+T|t+1}^* \in \mathcal{D}$, $\hat{n}_{t-L+1:t+1|t+1}^* \in \mathcal{N}$ such that

$$J_{t+1}^* = \min_{\hat{u}_{t+1:t+T|t+1} \in \mathcal{U}} J_{t+1}(\hat{x}_{t-L+1|t+1}^*, u_{t-L+1:t}, \hat{u}_{t+1:t+T|t+1}, \hat{d}_{t-L+1:t+T|t+1}^*, y_{t-L+1:t+1}). \quad (\text{A.2})$$

On the other hand, from Assumption 3 at time $t+T$, with $d = \hat{d}_{t+T|t+1}^*$ and

$$x = \hat{x}_{t+T|t+1}^* := \varphi(t+T; t-L+1, \hat{x}_{t-L+1|t+1}^*, \hat{u}_{t+1:t+T|t+1}^*, \hat{d}_{t-L+1:t+T|t+1}^*),$$

we conclude that there exists a control $\tilde{u}_{t+T} \in \mathcal{U}$ such that

$$q_{t+T+1}(f_{t+T}(\hat{x}_{t+T|t+1}^*, \tilde{u}_{t+T}, \hat{d}_{t+T|t+1}^*)) - q_{t+T}(\hat{x}_{t+T|t+1}^*) + c_{t+T}(\hat{x}_{t+T|t+1}^*, \tilde{u}_{t+T}, \hat{d}_{t+T|t+1}^*) - \rho_{t+T}(\hat{d}_{t+T|t+1}^*) \leq 0. \quad (\text{A.3})$$

Moreover, we conclude from Assumption 2, that there exist vectors $\tilde{x}_{t-L}, \tilde{d}_{t-L} \in \mathcal{D}$, $\tilde{n}_{t-L} \in \mathcal{N}$ such that

$$\begin{aligned} \hat{x}_{t-L+1|t+1}^* &= f_{t-L}(\tilde{x}_{t-L}, u_{t-L}, \tilde{d}_{t-L}), \\ y_{t-L} &= g_{t-L}(\tilde{x}_{t-L}) + \tilde{n}_{t-L}, \end{aligned} \quad (\text{A.4})$$

Using now (9a) in Assumption 1 at time t , we conclude that there also exists a finite scalar $J_t^* \in \mathbb{R}$ and a sequence $\hat{u}_{t:t+T-1|t}^* \in \mathcal{U}$ such that

$$J_t^* = \max_{\substack{\hat{x}_{t-L|t} \in \mathcal{X}, \\ \hat{d}_{t-L:t+T-1|t} \in \mathcal{D}, \\ \hat{n}_{t-L:t|t} \in \mathcal{N}}} J_t(\hat{x}_{t-L|t}, u_{t-L:t-1}, \hat{u}_{t:t+T-1|t}^*, \hat{d}_{t-L:t+T-1|t}, y_{t-L:t}). \quad (\text{A.5})$$

Going back to (A.2), we then conclude that

$$J_{t+1}^* \leq J_{t+1}(\hat{x}_{t-L+1|t+1}^*, u_{t-L+1:t}, \hat{u}_{t+1:t+T-1|t}^*, \tilde{u}_{t+T}, \hat{d}_{t-L+1:t+T|t+1}^*, y_{t-L+1:t+1}) \quad (\text{A.6})$$

because the minimization in (A.2) with respect to $\hat{u}_{t+1:t+T|t+1} \in \mathcal{U}$ must lead to a value no larger than what would be obtained by setting $\hat{u}_{t+1:t+T-1|t+1} = \hat{u}_{t+1:t+T-1|t}^*$ and $\hat{u}_{t+T|t+1} = \tilde{u}_{t+T}$.

Similarly, we can conclude from (A.5) that

$$\begin{aligned} J_t^* &\geq J_t(\tilde{x}_{t-L}, u_{t-L:t-1}, \hat{u}_{t:t+T-1|t}^*, \tilde{d}_{t-L}, \\ &\quad \hat{d}_{t-L+1:t+T-1|t+1}^*, y_{t-L:t}) \\ &= J_t(\tilde{x}_{t-L}, u_{t-L:t}, \hat{u}_{t+1:t+T-1|t}^*, \tilde{d}_{t-L}, \\ &\quad \hat{d}_{t-L+1:t+T-1|t+1}^*, y_{t-L:t}), \end{aligned} \quad (\text{A.7})$$

because the maximization in (A.5) with respect to $\hat{x}_{t-L|t}$ and $\hat{d}_{t-L:t+T-1|t}$ must lead to a value no smaller than what would be obtained by setting $\hat{x}_{t-L|t} = \tilde{x}_{t-L}$, $\hat{d}_{t-L|t} = \tilde{d}_{t-L}$ and $\hat{d}_{t-L+1:t+T-1|t} = \hat{d}_{t-L+1:t+T-1|t+1}^*$. The last equality in (A.7) is obtained by applying the control law (7).

Combining (A.6), (A.7), and (A.4) leads to

$$\begin{aligned} J_{t+1}^* - J_t^* &\leq J_{t+1}(f_{t-L}(\tilde{x}_{t-L}, u_{t-L}, \tilde{d}_{t-L}), u_{t-L+1:t}, \\ &\quad \hat{u}_{t+1:t+T-1|t}^*, \tilde{u}_{t+T}, \hat{d}_{t-L+1:t+T|t+1}^*, y_{t-L+1:t+1}) \\ &\quad - J_t(\tilde{x}_{t-L}, u_{t-L:t}, \hat{u}_{t+1:t+T-1|t}^*, \tilde{d}_{t-L}, \\ &\quad \hat{d}_{t-L+1:t+T-1|t+1}^*, y_{t-L:t}). \end{aligned} \quad (\text{A.8})$$

A crucial observation behind this inequality is that *both* terms $J_{t+1}(\cdot)$ and $J_t(\cdot)$ in the right-hand side of (A.8) are computed along a trajectory initialized at time $t-L$ with the *same initial state* \tilde{x}_{t-L} and share the *same control input* sequence $u_{t-L:t}, \hat{u}_{t+1:t+T-1|t}^*$ and the *same disturbance input* sequence $\tilde{d}_{t-L}, \hat{d}_{t-L+1:t+T-1|t+1}^*$. We shall denote this common state trajectory by \tilde{x}_s , $s \in \{t-L, \dots, t+T\}$, and the shared control and disturbance sequences by

$$\begin{aligned} \tilde{d}_s &:= \hat{d}_s^*|_{t+1}, \quad \forall s \in \{t-L+1, \dots, t+T-1\}, \\ \tilde{u}_s &:= \begin{cases} u_s & s \in \{t-L, \dots, t\} \\ \hat{u}_s^*|_t & s \in \{t+1, \dots, t+T-1\}. \end{cases} \end{aligned}$$

The vectors \tilde{u}_{t+T} and \tilde{d}_{t-L} have been previously defined, but we now also define $\tilde{d}_{t+T} := \hat{d}_{t+T}^*|_{t+1}$, $\tilde{x}_{t+T+1} := f_{t+T}(\tilde{x}_{t+T}, \tilde{u}_{t+T}, \tilde{d}_{t+T})$, and $\tilde{n}_s := y_s - g_s(\tilde{x}_s)$, $s \in \{t-L, \dots, t\}$. All of these definitions enable us to express

both terms $J_{t+1}(\cdot)$ and $J_t(\cdot)$ in the right-hand side of (A.8) as follows:

$$\begin{aligned}
J_{t+1}^* - J_t^* &\leq \sum_{s=t+1}^{t+T} c_s(\tilde{x}_s, \tilde{u}_s, \tilde{d}_s) + q_{t+T+1}(\tilde{x}_{t+T+1}) \\
&\quad - \sum_{s=t-L+1}^{t+1} \eta_s(\tilde{n}_s) - \sum_{s=t-L+1}^{t+T} \rho_s(\tilde{d}_s) \\
&\quad - \sum_{s=t}^{t+T-1} c_s(\tilde{x}_s, \tilde{u}_s, \tilde{d}_s) - q_{t+T}(\tilde{x}_{t+T}) \\
&\quad + \sum_{s=t-L}^t \eta_s(\tilde{n}_s) + \sum_{s=t-L}^{t+T-1} \rho_s(\tilde{d}_s) \\
&= c_{t+T}(\tilde{x}_{t+T}, \tilde{u}_{t+T}, \tilde{d}_{t+T}) + q_{t+T+1}(\tilde{x}_{t+T+1}) \\
&\quad - q_{t+T}(\tilde{x}_{t+T}) - \rho_{t+T}(\tilde{d}_{t+T}) + \eta_{t-L}(\tilde{n}_{t-L}) \\
&\quad + \rho_{t-L}(\tilde{d}_{t-L}) - c_t(\tilde{x}_t, \tilde{u}_t, \tilde{d}_t) - \eta_{t+1}(\tilde{n}_{t+1}).
\end{aligned}$$

Equation (A.1) follows from this, (A.3), and the fact that $c_t(\cdot)$ and $\eta_{t+1}(\cdot)$ are both non-negative. \blacksquare

With most of the hard work done, we are now ready to prove the main result of this section.

Proof of Theorem 1. Using (9a) in Assumption 1, we conclude that

$$\begin{aligned}
J_t^* &= \max_{\substack{\hat{x}_{t-L|t} \in \mathcal{X}, \\ \hat{d}_{t-L:t+T-1|t} \in \mathcal{D}, \\ \hat{n}_{t-L:t|t} \in \mathcal{N}}} \\
&\quad J_t(\hat{x}_{t-L|t}, u_{t-L:t-1}, \hat{u}_{t:t+T-1|t}^*, \hat{d}_{t-L:t+T-1|t}, y_{t-L:t}) \\
&\geq J_t(x_{t-L}, u_{t-L:t-1}, \hat{u}_{t:t+T-1|t}^*, d_{t-L:t}, 0_{t+1:t+T-1}, y_{t-L:t}) \\
&= J_t(x_{t-L}, u_{t-L:t}, \hat{u}_{t+1:t+T-1|t}^*, d_{t-L:t}, 0_{t+1:t+T-1}, y_{t-L:t}).
\end{aligned}$$

The first inequality is a consequence of the fact that the maximum must lead to a value no smaller than what would have been obtained by setting $\hat{x}_{t-L|t}$ equal to the true state x_{t-L} , setting $\hat{d}_{t-L:t}$ equal to the true (past) disturbances $d_{t-L:t}$ and setting $\hat{d}_{t+1:t+T-1}$ equal to zero. The final equality is obtained simply from the use of the control law (7).

To proceed, we replace $J_t(\cdot)$ by its definition in (5), while dropping all “future” positive terms in $c_s(\cdot)$, $s > t$ and $q_{t+T}(\cdot)$. This leads to

$$J_t^* \geq c_t(x_t, u_t, d_t) - \sum_{s=t-L}^t \eta_s(n_s) - \sum_{s=t-L}^t \rho_s(d_s). \quad (\text{A.9})$$

Note that the future controls $\hat{u}_{t+1:t+T-1|t}^*$ disappeared because we dropped all the (positive) terms involving

the value of the state past time t , and the summation over future disturbances also disappeared since we set all the future $\hat{d}_{t+1:t+T-1}$ to zero.

Adding both sides of (A.1) in Lemma 2 from time L to time $t-1$, leads to

$$J_t^* \leq J_L^* + \sum_{s=0}^{t-L-1} \rho_s(\tilde{d}_s) + \sum_{s=0}^{t-L-1} \eta_s(\tilde{n}_s), \quad \forall t \in \mathbb{Z}_{\geq L}. \quad (\text{A.10})$$

The bound in (13) follows directly from (A.9) and (A.10). \blacksquare

A.2 Proof of Lemma 1

Proof of Lemma 1. The proof is a direct consequence of the following sequence of inequalities that start from the equalities in (23c) and use the conditions (23a)-(23b), and the definitions (25) to arrive at (24):

$$\begin{aligned}
f(\hat{u}, \hat{d}) - \epsilon_f &= L_f(\hat{u}, \hat{d}, \hat{\lambda}_{fu}, \hat{\nu}_{fu}) - \hat{\nu}_{fu} G_u(\hat{u}, \hat{d}) \\
&= \min_{u \in \mathbb{R}^{N_u}} L_f(u, \hat{d}, \hat{\lambda}_{fu}, \hat{\nu}_{fu}) - 0 \\
&= \min_{u \in \mathbb{R}^{N_u}} f(u, \hat{d}) - \hat{\lambda}_{fu} F_u(u, \hat{d}) + \hat{\nu}_{fu} G_u(u, \hat{d}) \\
&\leq \max_{\lambda_{fu} \geq 0, \nu_{fu}} \min_{u \in \mathbb{R}^{N_u}} f(u, \hat{d}) - \lambda_{fu} F_u(u, \hat{d}) + \nu_{fu} G_u(u, \hat{d}) \\
&\leq \max_{\lambda_{fu} \geq 0, \nu_{fu}} \min_{u \in \mathcal{U}[\hat{d}]} f(u, \hat{d}) - \lambda_{fu} F_u(u, \hat{d}) + \nu_{fu} G_u(u, \hat{d}) \\
&= \min_{u \in \mathcal{U}[\hat{d}]} f(u, \hat{d}), \\
g(\hat{u}, \hat{d}) - \epsilon_g &= L_g(\hat{u}, \hat{d}, \hat{\lambda}_{gd}, \hat{\nu}_{gd}) - \hat{\nu}_{gd} G_d(\hat{u}, \hat{d}) \\
&= \min_{d \in \mathbb{R}^{N_d}} L_g(\hat{u}, d, \hat{\lambda}_{gd}, \hat{\nu}_{gd}) - 0 \\
&= \min_{d \in \mathbb{R}^{N_d}} g(\hat{u}, d) - \hat{\lambda}_{gd} F_d(\hat{u}, d) + \hat{\nu}_{gd} G_d(\hat{u}, d) \\
&\leq \max_{\lambda_{gd} \geq 0, \nu_{gd}} \min_{d \in \mathbb{R}^{N_d}} g(\hat{u}, d) - \lambda_{gd} F_d(\hat{u}, d) + \nu_{gd} G_d(\hat{u}, d) \\
&\leq \max_{\lambda_{gd} \geq 0, \nu_{gd}} \min_{d \in \mathcal{D}[\hat{u}]} g(\hat{u}, d) - \lambda_{gd} F_d(\hat{u}, d) + \nu_{gd} G_d(\hat{u}, d) \\
&= \min_{d \in \mathcal{D}[\hat{u}]} g(\hat{u}, d). \quad \blacksquare
\end{aligned}$$

References

- Alessandri, A., Baglietto, M., & Battistelli, G. (2008). Moving-horizon state estimation for nonlinear discrete-time systems: New stability results and approximation schemes. *Automatica*, 44(7), 1753–1765.
- Allgöwer, F., Badgwell, T. A., Qin, S. J., Rawlings, J. B., & Wright, S. J. (1999). Nonlinear predictive control and moving horizon estimation-an introductory overview. In *Advances in control* (pp. 391–449). Springer.
- Başar, T. & Olsder, G. J. (1995). *Dynamic Noncooperative Game Theory*. London: Academic Press.

- Bemporad, A., Borrelli, F., & Morari, M. (2003). Min-max control of constrained uncertain discrete-time linear systems. *Automatic Control, IEEE Transactions on*, 48(9), 1600–1606.
- Bemporad, A. & Morari, M. (1999). Robust model predictive control: A survey. In *Robustness in identification and control* (pp. 207–226). Springer.
- Betts, J. T. (2010). *Practical methods for optimal control and estimation using nonlinear programming*, volume 19. Siam.
- Biegler, L. T. (2000). Efficient solution of dynamic optimization and NMPC problems. In *Nonlinear model predictive control* (pp. 219–243). Springer.
- Biegler, L. T. (2013). A survey on sensitivity-based nonlinear model predictive control. *IFAC Proceedings Volumes*, 46(32), 499–510.
- Biegler, L. T. & Rawlings, J. B. (1991). Optimization approaches to nonlinear model predictive control. Technical report, Argonne National Lab., IL (USA).
- Boyd, S. P. & Vandenberghe, L. (2004). *Convex optimization*. Cambridge university press.
- Camacho, E. F. & Bordons, C. (2004). *Model predictive control*, volume 2. Springer London.
- Campo, P. J. & Morari, M. (1987). Robust model predictive control. In *American Control Conference, 1987*, (pp. 1021–1026). IEEE.
- Chen, H., Scherer, C. W., & Allgöwer, F. (1997). A game theoretic approach to nonlinear robust receding horizon control of constrained systems. In *Proceedings of the American Control Conference, 1997*, volume 5, (pp. 3073–3077). IEEE.
- Copp, D. A. & Hespanha, J. P. (2014). Nonlinear output-feedback model predictive control with moving horizon estimation. In *IEEE Conference on Decision and Control*, (pp. 3511–3517).
- Copp, D. A. & Hespanha, J. P. (2015). Nonlinear output-feedback model predictive control with moving horizon estimation: Illustrative examples. Technical report, Univ. California, Santa Barbara.
- Copp, D. A. & Hespanha, J. P. (2016a). Addressing adaptation and learning in the context of model predictive control with moving horizon estimation. In K. G. Vamvoudakis & S. Jagannathan (Eds.), *Control of Complex Systems: Theory and Applications* chapter 6. Elsevier.
- Copp, D. A. & Hespanha, J. P. (2016b). Conditions for saddle-point equilibria in output-feedback MPC with MHE. In *2016 American Control Conference (ACC)*, (pp. 13–19). IEEE.
- de la Peña, D. M., Alamo, T., Ramírez, D. R., & Camacho, E. F. (2007). Min-max model predictive control as a quadratic program. *Control Theory & Applications, IET*, 1(1), 328–333.
- Diehl, M. & Bjornberg, J. (2004). Robust dynamic programming for min-max model predictive control of constrained uncertain systems. *Automatic Control, IEEE Transactions on*, 49(12), 2253–2257.
- Diehl, M., Ferreau, H. J., & Haverbeke, N. (2009). Efficient numerical methods for nonlinear MPC and moving horizon estimation. In *Nonlinear Model Predictive Control* (pp. 391–417). Springer.
- Findeisen, R., Imsland, L., Allgöwer, F., & Foss, B. A. (2003). State and output feedback nonlinear model predictive control: An overview. *European journal of control*, 9(2), 190–206.
- Grant, M. & Boyd, S. (2008). Graph implementations for nonsmooth convex programs. In V. Blondel, S. Boyd, & H. Kimura (Eds.), *Recent Advances in Learning and Control*, volume 371 of *Lecture Notes in Control and Information Sciences* (pp. 95–110). Springer Berlin / Heidelberg.
- Grüne, L. & Pannek, J. (2011). *Nonlinear Model Predictive Control*. Springer.
- Huang, R., Patwardhan, S. C., & Biegler, L. T. (2009). Robust extended Kalman filter based nonlinear model predictive control formulation. In *Joint 48th IEEE Conference on Decision and Control and 28th Chinese Control Conference*, (pp. 8046–8051), Shanghai, P.R. China.
- Imsland, L., Findeisen, R., Bullinger, E., Allgöwer, F., & Foss, B. A. (2003). A note on stability, robustness and performance of output feedback nonlinear model predictive control. *Journal of Process Control*, 13(7), 633–644.
- Lazar, M., Muñoz de la Peña, D., Heemels, W. P. M. H., & Alamo, T. (2008). On input-to-state stability of min-max nonlinear model predictive control. *Systems & Control Letters*, 57(1), 39–48.
- Lee, J. H. & Yu, Z. (1997). Worst-case formulations of model predictive control for systems with bounded parameters. *Automatica*, 33(5), 763–781.
- Liberzon, D., Sontag, E. D., & Wang, Y. (2002). Universal construction of feedback laws achieving ISS and integral-ISS disturbance attenuation. *Systems & Control Letters*, 46(2), 111–127.
- Limon, D., Alamo, T., Raimondo, D. M., de la Peña, D. M., Bravo, J. M., Ferramosca, A., & Camacho, E. F. (2009). Input-to-state stability: a unifying framework for robust model predictive control. In *Nonlinear model predictive control* (pp. 1–26). Springer.
- Liu, J. (2013). Moving horizon state estimation for nonlinear systems with bounded uncertainties. *Chemical Engineering Science*, 93, 376–386.
- Löfberg, J. (2002). Towards joint state estimation and control in minimax MPC. In *Proceedings of 15th IFAC World Congress, Barcelona, Spain*.
- Magni, L., De Nicolao, G., Scattolini, R., & Allgöwer, F. (2003). Robust model predictive control for nonlinear discrete-time systems. *International Journal of Robust and Nonlinear Control*, 13(3–4), 229–246.
- Mayne, D. Q. (2014). Model predictive control: Recent developments and future promise. *Automatica*, 50(12), 2967–2986.
- Mayne, D. Q., Raković, S. V., Findeisen, R., & Allgöwer, F. (2006). Robust output feedback model predictive control of constrained linear systems. *Automatica*, 42(7), 1217–1222.
- Mayne, D. Q., Raković, S. V., Findeisen, R., & Allgöwer, F. (2009). Robust output feedback model predictive control of constrained linear systems: Time varying case. *Automatica*, 45(9), 2082–2087.
- Mayne, D. Q., Rawlings, J. B., Rao, C. V., & Scolaert, P. O. M. (2000). Constrained model predictive control: Stability and optimality. *Automatica*, 36(6), 789–814.
- Michalska, H. & Mayne, D. Q. (1995). Moving horizon observers and observer-based control. *IEEE Transactions on Automatic Control*, 40(6), 995–1006.
- Morari, M. & H Lee, J. (1999). Model predictive control: past, present and future. *Computers & Chemical Engineering*, 23(4), 667–682.
- Nesterov, Y. (2005). Smooth minimization of non-smooth functions. *Mathematical Programming*, 103(1), 127–152.
- Qin, S. J. & Badgwell, T. A. (2003). A survey of industrial model predictive control technology. *Control engineering practice*, 11(7), 733–764.
- Raimondo, D. M., Limon, D., Lazar, M., Magni, L., & Camacho, E. F. (2009). Min-max model predictive control of nonlinear systems: A unifying overview on stability. *European Journal of Control*, 15(1), 5–21.
- Rao, C. V., Rawlings, J. B., & Lee, J. H. (2001). Constrained linear state estimation—a moving horizon approach. *Automatica*, 37(10), 1619–1628.
- Rao, C. V., Rawlings, J. B., & Mayne, D. Q. (2003). Constrained state estimation for nonlinear discrete-time systems: Stability and moving horizon approximations. *Automatic Control, IEEE Transactions on*, 48(2), 246–258.
- Rao, C. V., Wright, S. J., & Rawlings, J. B. (1998). Application of interior-point methods to model predictive control. *Journal of optimization theory and applications*, 99(3), 723–757.

- Rawlings, J. B. (2000). Tutorial overview of model predictive control. *Control Systems, IEEE*, 20(3), 38–52.
- Rawlings, J. B. & Bakshi, B. R. (2006). Particle filtering and moving horizon estimation. *Computers & chemical engineering*, 30(10), 1529–1541.
- Rawlings, J. B. & Mayne, D. Q. (2009). *Model Predictive Control: Theory and Design*. Nob Hill Publishing.
- Roset, B., Lazar, M., Nijmeijer, H., & Heemels, W. (2006). Stabilizing output feedback nonlinear model predictive control: An extended observer approach. In *Proc. of the 17th International Symposium on Mathematical Theory of Networks and Systems*, (pp. 771–781).
- Scokaert, P. O. M. & Mayne, D. Q. (1998). Min-max feedback model predictive control for constrained linear systems. *Automatic Control, IEEE Transactions on*, 43(8), 1136–1142.
- Sontag, E. D. (1999). Control-lyapunov functions. In *Open problems in mathematical systems and control theory* (pp. 211–216). Springer.
- Sui, D., Feng, L., & Hovd, M. (2008). Robust output feedback model predictive control for linear systems via moving horizon estimation. In *American Control Conference, 2008*, (pp. 453–458). IEEE.
- Vandenberghe, L. (2010). The CVXOPT linear and quadratic cone program solvers. Technical report, Univ. California, Los Angeles.
- Wang, Y. & Boyd, S. (2010). Fast model predictive control using online optimization. *Control Systems Technology, IEEE Transactions on*, 18(2), 267–278.
- Wright, S. J. (1997a). Applying new optimization algorithms to model predictive control. In *AICHE Symposium Series*, volume 93, (pp. 147–155).
- Wright, S. J. (1997b). *Primal-dual interior-point methods*, volume 54. Siam.
- Zhang, J. & Liu, J. (2013). Lyapunov-based MPC with robust moving horizon estimation and its triggered implementation. *AICHE Journal*, 59(11), 4273–4286.